

Numerical Analysis of Compressive Flow and Fracture Toughness of Aluminum Powder Compacts

Mohammed Y. Abdellah^{1,3,*}, Nadia E. Bondok^{2,4}, Hamza A. Ghulman³

¹Mechanical Engineering Department, Faculty of Engineering, South Valley University, Qena

²Department of technology Development, Specified Studies Academy, Worker's University, Cairo, Egypt

³Mechanical Engineering Department, Collage of Engineering and Islamic Architecture, Umm Al-Qura University Makkah, KSA

⁴Interior Design Department, Faculty of Design and Architecture, Jizan University, Saudi Arabia

*Corresponding author: Mohammed_yahya42@yahoo.com

Abstract The finite element analysis (FEA) has become an effective way to numerically simulate strength distribution in a powder metallurgy (P/M) compact. A 2-D Finite element model is carried out to simulate the flow behaviours of green aluminium powder compacts. The complicated case of green aluminium powder makes it is difficult from metalwork point of view to get analytical or empirical model to predict the compacts strength. Therefore, Cold Compression test is simulated using the 2-d model with ABAQUS software for compacted aluminium plate. Moreover, fracture toughness of the compacted aluminium powder is calculated using 2- D J-integral finite element model implemented into ABAQUS commercial. The results are in good agreement with the experimental ones and give a valuable graph decrypting the flow behaviour of the green compacts. The calculated fracture toughness of compacted aluminium powder is nearly $150 MPa\sqrt{m}$.

Keywords: J-integral, Compact tension, powder metallurgy, Finite element

Cite This Article: Mohammed Y. Abdellah, Nadia E. Bondok, and Hamza A. Ghulman, "Numerical Analysis of Compressive Flow and Fracture Toughness of Aluminum Powder Compacts." *American Journal of Materials Engineering and Technology*, vol. 4, no. 2 (2016): 16-21. doi: 10.12691/materials-4-2-1.

1. Introduction

A great variety of engineering application found in aluminium and its alloy due to their unconventional properties. Mechanical properties are distinguished by light weight to strength [1].

Hassan et al. [3] studied effect of ceramic additives on aluminium alloy 6061 using casting technology. They concluded that increasing of ceramic additives increase compressive strength and give good relative tribological behaviour.

Cunningham et al. [4] build an analytical (continuum approach) on ceramic, and pharmaceutical powders. Another study used FE modelling in ABAQUS to compare several available material models to the model based on Al-6061 alloy powder in both cold isostatic pressing and die compaction [5].

Ranjit et al. [6] simulated the compaction process to achieve uniform and high bulk density green parts (parts do not have sintered yet). A material model (Cam-Clay) which can capture the particle re-arrangement under compaction process has been adopted. An axi-symmetric analysis has been followed on 601AB aluminium alloy powder with initial apparent density as 40%.

Finite element method simulation for a torsional upset forging process [7] is carried out. Stress and strain distribution and forging load are obtained experimentally and compared with the finite element model. It is observed that magnitude of non-homogeneous deformation, dead

metal zone and upset force, are decrease because the friction factor and rotation speed are increased.

K.T Kim and J.H Cho [8] investigated the consolidation behaviour of mixed copper and tool steel powder under cold compaction process using Finite element analysis. The results showed that the yield functions mixed by the fraction of contact implemented in finite element analysis agreed better than those by volume fractions of Cu powder with experimental data.

Fleck [9] developed a constitutive model for Stage I cold compaction of powders under general loading. The evolution of anisotropy under general loading was described using an internal state variable model. The results were in good agreement with the experimental observation.

Martin et al. [10] used discrete element models (DEM) for powder compaction. They showed that DEM results were consistent with micromechanical models for isostatic loading, as the shear strain is increased, but with differences occurring. Many other models [11-16] investigate the powder compaction techniques and effect of compaction parameters.

Mohammed et al. [17] investigated the wear properties of hot extruded reinforced aluminium powder compacted at elevated temperature while the mechanical characteristics were investigated in [18].

Korim et al. [19] investigated the porous titanium mechanical properties using crushable finite element model. The results were in good agreement with the published experimental data.

Mohammed et al. [20] studied fracture toughness of compacted layered material. It was achieved that FE was a good technique to simulate fracture toughness of layered material.

Y. Mohammed et al. [21] constructed FE simulation to model flow behaviour of reinforced aluminium powder compacts. The results were accurate good.

The aim of the present study is to measure compressive strength of green aluminum powder compacts and its cold fracture toughness.

2. Material Behavior and Characterization

A commercial aluminium metal powder with a mean size of 80 grit/inch supplied by ADWIC code number 8010075, molecular weight of 26.98 is used for all specimens as a matrix (base material). Figure 1 shows the



Figure 1. Photograph illustrate powder particles under optical macroscopic (x40)

Table 1. Mechanical properties of the tested materials

Test Material	Compaction velocity, mm/min	Modulus of Elasticity, GPa	Yield strength, MPa	Ultimate strength
Aluminium	5	500	53.56	92

The compaction velocity was 5 mm/min. The process continues to the maximum compaction load value then the load is released. The details of the manufacturing process are not the study case and it is completely described in [18].

To know how the materials, behave under loading, compression test is carried out to obtain the engineering stress-strain curves of the aluminium powder compacts. Figure 2 illustrates the experimental data. The true stress-strain curves and the described true stress/plastic strain are used in FEM - domains. The compression test is carried out at 5mm/min.

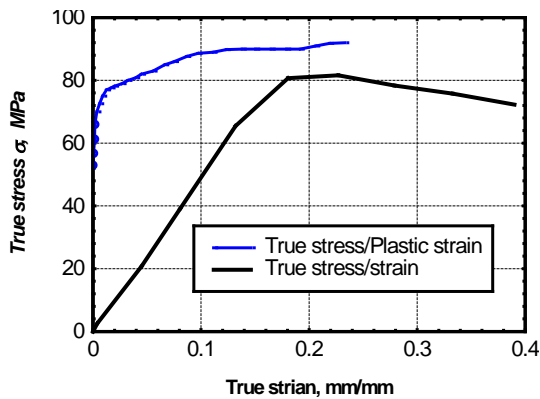


Figure 2. True stress–strain curves of Al-powder compacted

The mechanical properties for the tested materials at compaction velocity (5mm/min), which were extracted from the previous figures, can be summarized in Table 1.

The Bauschinger effect is commonly ignored in plastically theory, and is usual to assume that the yield stress in tension and compression are the same [22].

3. Constitutive Equations

Generally, there are several options available for describing the plasticity behaviour. These options can be classified to bilinear kinematics hardening, multilinear kinematics hardening and nonlinear kinematics hardening. The Bilinear Kinematic Hardening (BKIN) option

powder particles shape. Table 1 shows the mechanical properties of the used compacted aluminium plates.

(Figure 3 a) assumes the total stress range is equal to twice the yield stress, so that the Bauschinger effect is included. This option is recommended for general small-strain use for materials that obey von Mises yield criteria (which includes most metals). It is not recommended for large-strain applications. The Multilinear Kinematic Hardening (KINH and MKIN) options (Figure 3 b) use the Besseling model, also called the sub-layer or overlay model, so that the Bauschinger effect is included. KINH is preferred for use over MKIN because it allows you to define more stress-strain curves (40 vs. 5). The Nonlinear Kinematic Hardening (CHABOCHE) option uses the Chaboche model, which is a multi-component nonlinear kinematic hardening model that allows you to superpose several kinematic models [23]. Then the above options constitute the practical ways to represent the hardening law, which can be obtained, from the compression curve-for Al-compacts or tension curve for copper wires defined point by point can be used as in the present cases in this work. Stress-strain data representing the material hardening behavior are necessary to define the model. An experimental hardening curve might appear as that shown in Figure 2. Plastic strain values, not total strain values, are used in defining the hardening behaviour.

The simplest form of linear elasticity is the isotropic case, and the stress-strain relationship is given the following strain tensors Eqn. [24].

$$\begin{Bmatrix} \varepsilon_{11} \\ \varepsilon_{22} \\ \varepsilon_{33} \\ \varepsilon_{12} \\ \varepsilon_{13} \\ \varepsilon_{23} \end{Bmatrix} = \begin{bmatrix} 1/E & -\nu/E & -\nu/E & 0 & 0 & 0 \\ -\nu/E & 1/E & -\nu/E & 0 & 0 & 0 \\ -\nu/E & -\nu/E & 1/E & 0 & 0 & 0 \\ 0 & 0 & 0 & 1/G & 0 & 0 \\ 0 & 0 & 0 & 0 & 1/G & 0 \\ 0 & 0 & 0 & 0 & 0 & 1/G \end{bmatrix} \begin{Bmatrix} \sigma_{11} \\ \sigma_{22} \\ \sigma_{33} \\ \sigma_{12} \\ \sigma_{13} \\ \sigma_{23} \end{Bmatrix} \quad (1)$$

The elastic properties are completely defined by giving the Young's modulus E , and the Poisson's ratio ν . The shear modulus G , can be expressed in terms of E and ν as

$$G = \frac{E}{2(1+\nu)} \quad (2)$$

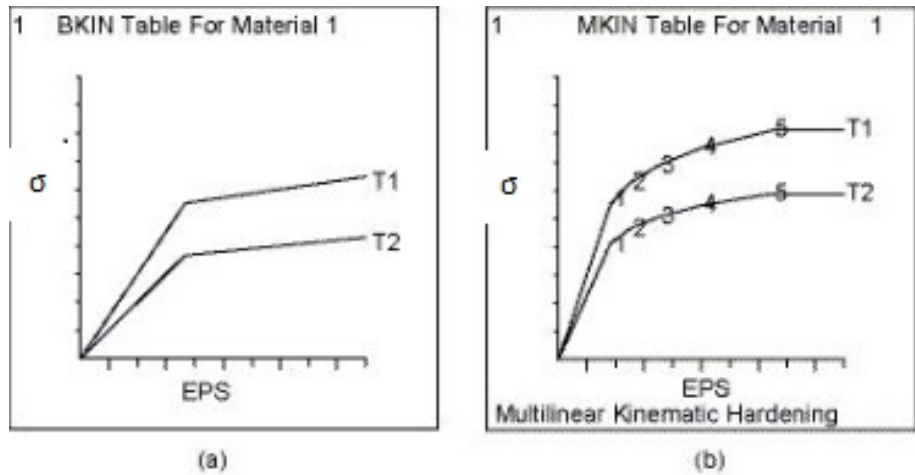


Figure 3. Kinematic Hardening(a) Bilinear kinematic hardening, (b) Multilinear kinematic hardening [26]

For large deformations, the first Piola-Kirchhoff stress tensors is suitable;

$$P = J \sigma \cdot F^{-T} \tag{3}$$

Where F is the deformation gradient and J is the Jacobian determine.

$$\sigma_{ij} = C_{ijkl} \varepsilon_{kl}^n \tag{4}$$

Where C_{ijkl} is the fourth order elastic modulus.

For simplicity, the present work simulation is in two directions, and assuming isotropic elasto-plastic solid. Thus, the complete model of that solid which subject to compressive uniaxial loading is the following [25,27]:

$$\varepsilon = \varepsilon_e + \varepsilon_p \tag{5}$$

$$\varepsilon_e = \sigma / E \tag{6}$$

$$\varepsilon_p = \frac{\sigma^n}{K_y} \tag{7}$$

Where (n) is the material hardening coefficient, K_y shear yield stress.

4. F. E-domain Structure

4.1. Compression Model

For building of F. E programs, there are main points must be clearly defined to make a real or good simulation like which is the problem state plain stress or plain strain, element type, material law for the both fibre and matrix materials, boundary conditions, etc. For simplicity, a 2-D problem was chosen with plain stress state. In addition, an axisymmetric domain was used due to its homogeneity about the axes. The axisymmetric mesh, which is used for networking a test specimen with 24 mm diameter and 12 mm height, an 8-node biquadratic plane stress quadrilateral, reduced integration (CPS8R) was chosen. CPS8R is used for 2-D modeling of solid structures, it provides more accurate results for the meshes and it can tolerate irregular shapes without as much loss of accuracy. The element is defined by eight nodes having two degrees of freedom at each node: translations in the nodal x and y directions as shown in Figure 4 the element has plasticity,

creep, swelling, stress stiffening, large deflection, and large strain capabilities. The number of elements was reached to 624 elements for the axisymmetric meshes. Figure 5 indicates the position of the used boundary conditions. The lower platen was fully fixed, while the upper platen was fixed in the x-direction only. The load i.e. displacement was applied in y-direction of the upper platen. As well as, the materials were defined in the F. E-program through the true stress- true plastic strain curve, which plotted in Figure 2. Friction between platen specimen interfaces was defined as a pair of contact body of constant friction coefficient equal to 0.1.

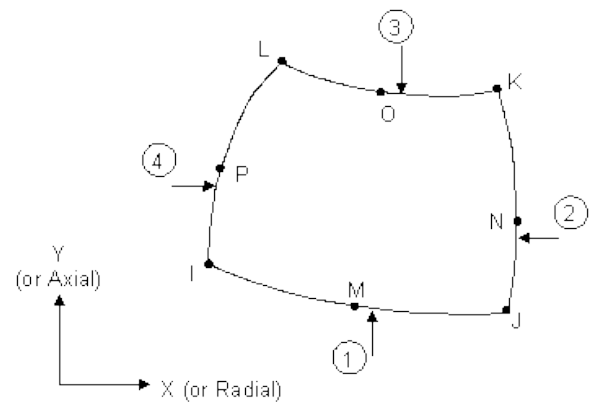


Figure 4. Eight-node biquadratic plane stress quadrilateral element [23]

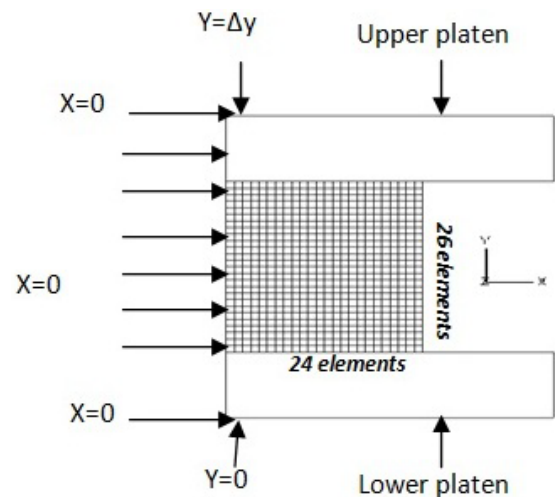


Figure 5. FE domain with mesh and boundary conditions

4.2. J-Integral FEM

Compact tension test specimen configuration is used according to ASTM D 5045 [23]. For complete description of the test return to [20]. A 2-D FEM of A 4-node bilinear plane strain quadrilateral, reduced integration, hourglass control (CPE4R) is implemented. The FEM domain is shown in Figure 6 a with partition region A and B and C. The total mesh domain of 624 elements is distributed in case that denser and refine meshes of 90 elements are in region A around crack tip. While rest of elements in other specimen regions B, C are

coarser (See Figure 6 b). meshing is used swept meshing technique to generate uniform mesh shape. Seam crack (crack can be separate) is insert in the FE domain with singularity of \sqrt{r} . The loading pins interacts with the specimen holes using tangential behaviour criteria of coefficient of friction equal 0.5. the loading pins is selected as discrete rigid wires. The model with interactions are shown in Figure 7 a. The history output is let to calculate J-integral for 5 contours. The boundary conditions are illustrated in (Figure 7 b).

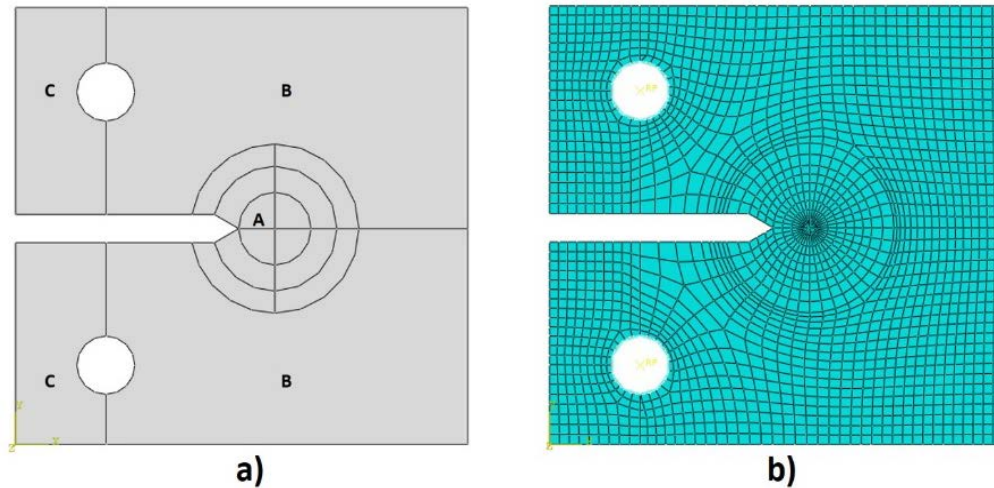


Figure 6. FEM domain a) part domain, b) Mesh domain

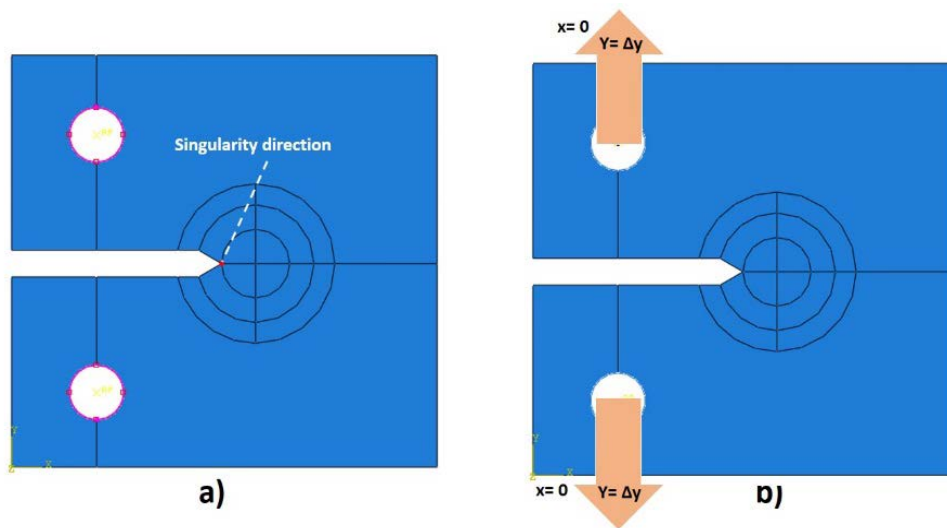


Figure 7. FE domain a) interaction, b)B. C

5. Results and Discussion

The Finite element simulation is performed to predict flow curve compared with the corresponding experimental ones and the stresses and strains contours also indicated. The program subroutine is controlled to stop at the beginning of failures for all examined specimens. Figure 8 examine whether the F.E M predicts well the compressive strength of aluminium powder compacts. It is observed clearly that the finite element method is reasonably agreed with experimental data and it should be noted that there it should be note the flow behavior extended to the failure

strain due to damage criteria of hardening material plasticity implemented into the FE subroutine. which give good deference between that in other workers [21]. In addition, case of friction is not the same in the experimental as the coefficient of friction in the calculation was assumed to be equal 0.1.

The deformed shapes are shown in Figure 9, while Von-Mise contours are shown in Figure 10. The barrel shape is shown, no damage fracture occurs, there is a harmful shear band extended from the centre of the specimens to the outer surface, especially with increase of reinforcement and it is increasing for specimens compacted at higher compaction velocity, this is due to stress concentration.

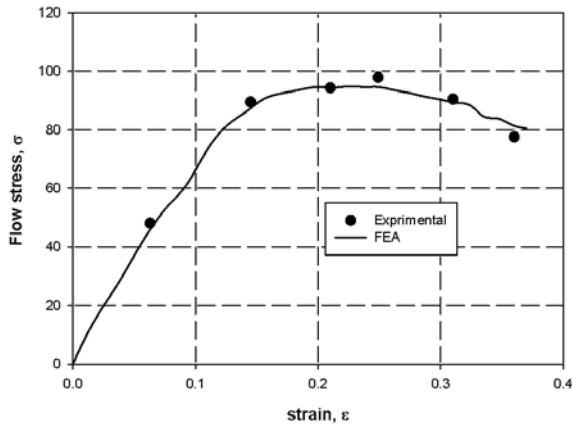


Figure 8. Comparing true stress-strain curve for Al- compacts

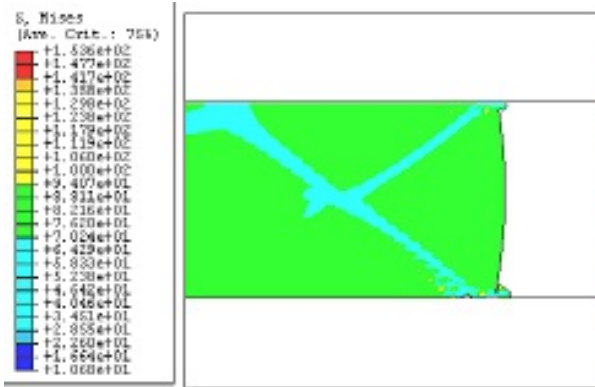


Figure 9. Von Mises stress for Al - powder compacts

The surface release energy (G_{IC}) which is an indication for fracture toughness (K_{IC}), which is measured using FE J-integral model curve which is shown in Figure 10. Implementing the obtained value (50 J/mm^2) in Eqn 8

$$K_{IC} = \sqrt{EG_{IC}} \tag{8}$$

The fracture toughness can be measured as $150 \text{ MPa} \sqrt{\text{m}}$. The contour fracture is mode I (opening mode) illustrated in Figure 11.

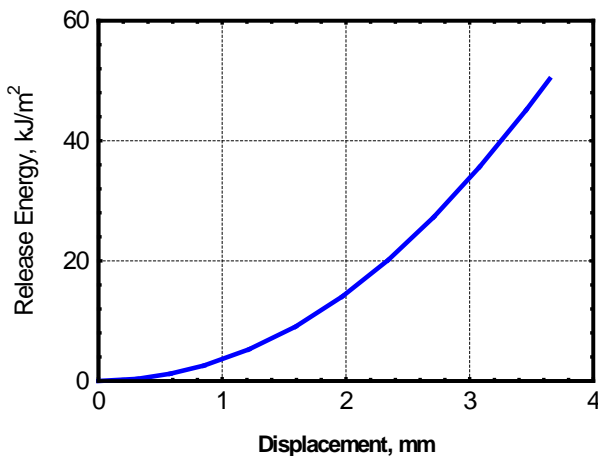


Figure 10. FE predicted J-integral

6. Conclusion

Finite element model is an accurate technique to simulate metal working process. Compression flow behaviours have been simulated in very acceptable results.

The cracks and damage failure are predicted in high degree of accuracy. Mode I fracture mechanics is achieved through J-integral FE analysis, with accurate degree fracture toughness is measured as $150 \text{ MPa} \sqrt{\text{m}}$.

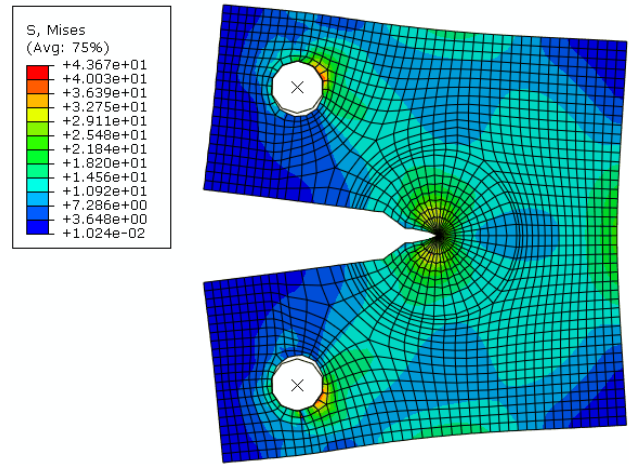


Figure 11. Von-Mises of mode I fracture

References

- [1] W.H. Hunt, New directions in aluminum-based P/M materials for automotive applications, International Journal of Powder Metallurgy 36, Pp. 50-56, 2000.
- [2] Sridhar, I., and N. A. Fleck. "Yield behaviour of cold compacted composite powders." Actamaterialia 48.13, Pp. 3341-3352, 2000.
- [3] Mohamed. K. Hassan, Y. Mohammed, Abu El-Ainin H. Improvement of Al-6061 alloys mechanical properties by controlling processing parameters. International Journal of Mechanical & Mechatronics Engineering IJMME-IJENS Vol: 12 Issue: 02 pp.14-18, 2012.
- [4] Cunningham, J. C., Sinka, I. C., Zavaliangos, A.. Analysis of Tablet Compaction. I. Characterization of Mechanical Behavior of Powder and Powder/Tooling Friction. Journal of Pharmaceutical Sciences, 93,Pp. 2022-39, 2004.
- [5] Lee, S. C., Kim, K. T.. Densification behavior of aluminum alloy powder under cold compaction. International Journal of Mechanical Sciences, 44(7), 1295-1308, Pp. 2002.
- [6] Verma, Ranjit Kumar, N. S. Mahesh, and M. I. Anwar. "Numerical Analysis of Powder Compaction to Obtain High Relative Density in '601AB'Aluminum Powder." SASTECH, Volume 11, Issue 1, Apr 2012.
- [7] Youn, S., et al. "Aluminium powder forging process using a rotating platen." Aluminium alloys: their physical and mechanical properties: proceedings of the 9th International Conference on aluminium alloys (ICAA9). Deakin University, School of Engineering and Technology, 2011.
- [8] Kim, K.. "A densification model for mixed metal powder under cold compaction", International Journal of Mechanical Sciences, 2001.
- [9] Fleck, N. A. "On the cold compaction of powders." Journal of the Mechanics and Physics of Solids 43.9, Pp. 1409-1431, 1995.
- [10] Martin, C. L., D. Bouvard, and S. Shima. "Study of particle rearrangement during powder compaction by the discrete element method." Journal of the Mechanics and Physics of Solids 51.4, Pp. 667-693, 2003.
- [11] Fleck, N. A., B. Storåkers, and R. M. McMeeking. "The viscoplastic compaction of powders." IUTAM Symposium on Mechanics of Granular and Porous Materials. Springer Netherlands, 1997.
- [12] Sinka, I. C. "Modelling powder compaction." Kona 25 (2007): 4.
- [13] Choi, J. L., and D. T. Gethin. "A discrete finite element modelling and measurements for powder compaction." Modelling and Simulation in Materials Science and Engineering 17.3, Pp. 035005, 2009.

- [14] Shang, C., I. C. Sinka, and J. Pan. "Constitutive Model Calibration for Powder Compaction Using Instrumented Die Testing." *Experimental mechanics* 52.7, Pp. 903-916, 2012.
- [15] Cocks, A. C. F., et al. "Compaction models." *Modelling of Powder Die Compaction*. Springer London, Pp. 43-64, 2008.
- [16] Schmidt, I., et al. "Simulation of the material behaviour of metal powder during compaction." *Proceedings of the Institution of Mechanical Engineers, Part E: Journal of Process Mechanical Engineering* 224.3, Pp. 187-194, 2010.
- [17] Mohammed Y. Abdellah, M. Mahmoud Moustafa, Ashraf T. Mohamed, G. T. Abdel-Jaber, *Wear Properties of Hot Extruded Aluminum Powder Compacts*, Open Access Library Journal, 2014, PP. 1-6.
- [18] Abdellah, M. Y., Moustafa, M. M., & Mohamed, A. T. *Hot Extrusion of Reinforced Aluminum Powder Compacts*. *International Journal of Materials Lifetime*, 1(1), 2014, 1-6.
- [19] N. S. Korim, M. Y. Abdellah, M. Dewidar and A. M. Abdelhaleem, "Crushable Finite Element Modeling of Mechanical Properties of Titanium Foam," *International Journal of Scientific & Engineering Research*, vol. 6, no. 10, pp. 1221-1227, 2015.
- [20] Y. Mohammed, M. K. Hassan and A. M. Hashem, "Finite Element Computational Approach of Fracture Toughness in Composite Compact Tension Specimen," *International Journal of Mechanical & Mechatronics Engineering*, vol. 12, no. 4, pp. 57-61, 2012.
- [21] Mohammed, Y., Moustafa, M.M., Mohamed, A.T. and Abdel-Jaber, G.T. (2014) *Finite Element Analysis of Flow Behaviors of Aluminum Powder Compacts*. *IJARES International Journal of Applied Research in Engineering and Science*, 1, 1-10.
- [22] G. E. Dieter, "Mechanical Metallurgy", McGraw Hill Book Co., 1988.
- [23] Ansys software 5.6.2, "tutorial".
- [24] ABAQUS, Version "6.9 Documentation.", Providence, RI: Dassault Systemes Simulia Corporation, 2009.
- [25] C. S. Kanga, S. C. Leea, K. T. Kima, and O. Rozenberg, "Densification behaviour of iron powder during cold stepped compaction", *Materials Science and Engineering, A* 452-453, pp. 359-366, 2007.
- [26] J. Lemaitre and J. L. Chaboche, "Mechanics of solid materials", Cambridge University press, translated by B. Shrivastava, pp. 168-169, 1990.
- [27] Astm, "D 5045-96, Standard Test Method for Plane-Strain Fracture Toughness and Strain Energy Release Rate of Plastic Materials.", Philadelphia: American Society for Testing and Materials, 199.